Shahrekord University

Journal of Microfluidic and Nanofluidic Research

Journal homepage: https://jmnr.sku.ac.ir

Research Article

Entropy Analysis in a Heat Sink with Laminar Fluid Flow Regime: A Numerical Investigation

Ahmad Najafpour [a]*, Alireza Khalili [b]

[a] *Department of Mechanical Engineering, Babol Noshirvani University of Technology, Babol, Iran*
[b] *Department of Energy Engineering, Sharif University of Technology, Tehran, Iran*

ARTICLE INFO

Article history:

Received: 2025-02-20

Revised: 2025-03-19

Accepted: 2025-03-20

Keywords:

Minichannel heat sink;
Entropy generation;
Thermal management;
CFD.

ABSTRACT

Thermal management in electrical appliances has a great impact on their performance and can reduce energy consumption. Heat sinks are an effective tool for cooling electrical equipment that can be used. In the present work, the entropy generation at Reynolds numbers (Re) = 200 to 1000 for 5 configurations of heat sinks with a constant heat flux of 20 kW/m^2 has been investigated, which can be effective in reducing the temperature of electrical devices. The results obtained show that with increasing Re, the amount of entropy generated due to fluid flow (S_p) is increased and the amount of entropy generated due to heat transfer (S_t) is decreased, and finally, increasing Re reduces entropy generation and improves system performance. At Re = 200, the S_t for Case 4 is decreased by 59.86%, 41.83%, 2.45%, and 2.74%, respectively, compared to the base case, Case 1, Case 2, and Case 3. At Re = 1000, the amount of N_a in Case 1, Case 2, Case 3, and Case 4 is decreased by 33.36%, 53.47%, 53.97%, and 55.66%, respectively.

1. Introduction

With the growth of industries, rising energy demand, and advancements in electronic technologies, the global use of energy production systems, energy storage solutions, and electronic devices has significantly increased. Nonetheless, the efficient operation and continued development of these technologies largely depend on effective thermal management and temperature regulation [1]. To ensure effective thermal management and reliable operation, several techniques have been employed, including air cooling [2], liquid cooling [3-5], and phase change cooling [6]. Among these, micro/mini-channel heat sinks (MCHSs) have emerged as a promising solution for thermal regulation in a range of applications, such as solar photovoltaic cells (PVCs) [7] and electronic devices [8]. While MCHSs can be integrated with both air and liquid cooling systems, the liquid-cooled variants have gained significant attention due to their superior heat dissipation performance. A variety of fluids, including water, oil, and ethylene glycol, can serve as coolants in these systems. Gannasegaran et al. [9] investigated how different geometrical configurations affect the thermal performance of microchannel heat sinks. They analyzed microchannels with three shapes—triangular, rectangular, and trapezoidal—each with three distinct size variations. The findings revealed that microchannels with smaller hydraulic diameters achieved superior heat transfer coefficients (HTCs) and better temperature uniformity. Among the shapes studied, the rectangular channel with the smallest hydraulic diameter

* **Corresponding author.**
E-mail address: amdnajafpour@gmail.com

Cite this article as:

Najafpour, A. and Khalili, A., 2025. Entropy Analysis in a Heat Sink with Laminar Fluid Flow Regime: A Numerical Investigation. *Journal of Microfluidic and Nanofluidic Research*, 1(2), pp. 65-71.

https://doi.org/10.22034/jmnr.2025.15169.1009

exhibited the highest HTC, followed by trapezoidal and then triangular geometries. Najafpour and el. [10] investigated the effect of changes in cross-sectional area in a mini-channel heat sink. Their study at Re 831 to 1496 showed that with increasing Re, the convection heat transfer coefficient increased and the thermal resistance decreased. By adding TiO_2, MgO and GO nanoparticles at volume fractions of 0.01, 0.03, and 0.05, the heat sink temperature decreased and the thermal resistance decreased compared to pure water. Ghadhban and Jaffal [11] explored the impact of different channel geometries—wave-shaped, S-shaped, and arc-shaped—on the performance of heat sinks. Their results showed that these modified shapes improved the Nusselt number by 30.5%, 18.7%, and 10.8%, respectively, compared to the standard straight channel design. Additionally, the arc-shaped channel demonstrated the most favorable ΔP, reducing it by 16% relative to the conventional configuration. Al-Hassani and Freegah [12] explored multiple factors to enhance the hydrothermal performance of serpentine microchannel heat sinks (MCHSs). They examined various configurations, including a double outlet design, channels with three different backward angles for secondary flow, and a hybrid model combining pin fins with secondary flow. Their study aimed to evaluate the impact of each configuration on key parameters such as the Nusselt number, ΔP, and thermal resistance. Najafpour et al. [13] proposed 5 multi-branch channel configurations for the heat sink. In the study, a constant heat flux of 26.67 kW/m^2 was introduced to the bottom of the heat sink and a fluid with a temperature of 300 K entered the heat sink. The results showed that Case 2 had the best performance among the proposed cases. In all cases, by increasing the Reynolds number from 100 to 300, 500, 700 and 900, the ΔP increased and the thermal resistance decreased. By employing triple hybrid nanoparticles, the Nusselt number decreased and the ΔP increased. In another study, Najafpour and Rostami [14] investigated fin-based heat sinks. Their work included five 60-degree heat sinks with a solid region made of copper and a fluid interface made of water. They investigated the effect of fin angle on heat sink performance, and their results showed that Case 3 with a 60-degree fin angle performed best among the proposed cases. Case 3 performed 26% and 40% better than the base case at Reynold number 800 and Reynolds number 1600, respectively. Fins with an angle of 60 (Case 3) produced the lowest thermal resistance and the angle of 90 (Case 4) produced the highest ΔP.

In this study, the entropy generation in a heat sink with a fin-based configuration for better cooling is analyzed. The employment of fins increases the contact area between the solid and the fluid, which can improve the cooling in the heat sink. This study also investigates the effect of geometric parameters such as the shape of the fin on the performance of the heat sink.

2. Numerical methodology

2.1. Geometric Shape and boundary conditions

In the present work, 5 geometries for mini-channel heat sinks are proposed, whose dimensions are (28×10×3) mm^3. The proposed cases have two solid domains of copper and a fluid domain of water, whose thermophysical properties are given in Table 1.

Table 1. Material properties [14].

Material	Water	Copper
ρ (kg/m3)	997	8933
c_p (J/kg.K)	4179	385
k (W/m.K)	0.6	401
μ (kg/m.s)	0.001	-

In all cases, a constant heat flux of 20 kW/m^2 is introduced to the bottom of the heat sink, and the cross-sectional area of the flow channels is (2×2) mm^2, where the fluid enters the flow channel with a constant temperature of 300 K, and a zero static pressure condition is assumed at the end of the channel (Fig. 1).

The proposed cases have two inlets with a D_h = 2 mm, through which the fluid enters the flow channel at a constant temperature and, after cooling, exits the channel through two outlets at the end of the channel. The base case is considered without fins, and Case 1, Case 2, Case 3, and Case 4 have fins with a special configuration to examine the effect of geometric changes in the fins on cooling and heat sink performance (Fig. 2).

2.2. Governing equations

In order to solve the governing equations for the current study, several simplifying assumptions have been made to facilitate the mathematical modeling and computational analysis. These assumptions are essential for making the problem tractable while preserving an acceptable level of accuracy.

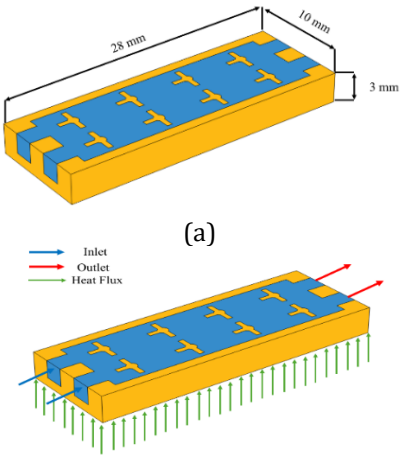

Fig. 1. (a) Geometric size of the heat sink. (b)The boundary conditions.

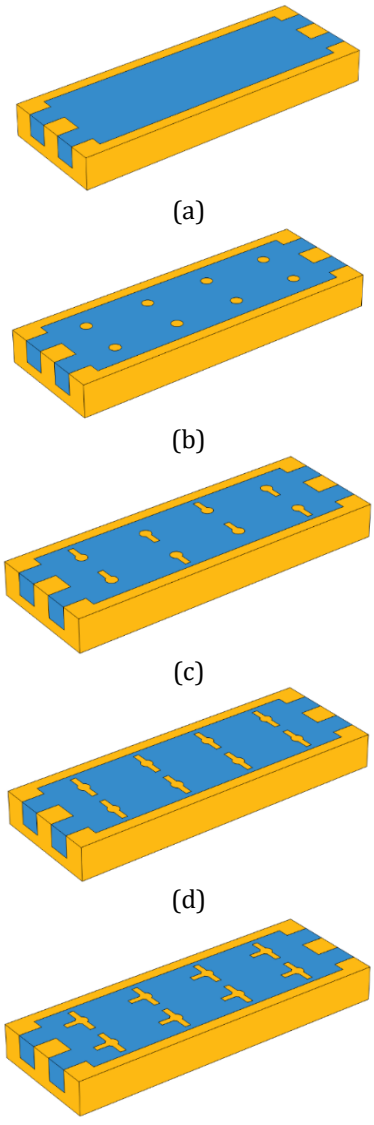

Fig. 2. Configuration of proposed geometries; a) base case, b) case 1, c) case 2, d) case 3 and e) case 4

The main assumptions are as follows:

- Material properties are assumed to remain constant and are not affected by temperature variations.
- The fluid flow is considered laminar and incompressible.
- Gravity effects and natural convection heat transfer are neglected in this study to simplify the model and concentrate on forced convection behavior.
- A uniform heat flux is applied to the bottom surface of the heat sink.
- Heat transfer by radiation is considered insignificant and thus omitted.

The fluid flow is governed by the continuity, momentum, and energy equations. The continuity equation is given as follows:

$$\frac{\partial u}{\partial x}+\frac{\partial v}{\partial y}+\frac{\partial w}{\partial z}=0 \quad (1)$$

Momentum equation:

X-momentum:

$$u\frac{\partial u}{\partial x}+v\frac{\partial u}{\partial y}+w\frac{\partial u}{\partial z}=-\frac{1}{\rho_f}\frac{\partial p}{\partial x}+\frac{\mu_f}{\rho_f}\left[\frac{\partial^2 u}{\partial x^2}+\frac{\partial^2 u}{\partial y^2}+\frac{\partial^2 u}{\partial z^2}\right] \quad (2)$$

Y-momentum:

$$u\frac{\partial v}{\partial x}+v\frac{\partial v}{\partial y}+w\frac{\partial v}{\partial z}=-\frac{1}{\rho_f}\frac{\partial p}{\partial y}+\frac{\mu_f}{\rho_f}\left[\frac{\partial^2 v}{\partial x^2}+\frac{\partial^2 v}{\partial y^2}+\frac{\partial^2 v}{\partial z^2}\right] \quad (3)$$

Z-momentum:

$$u\frac{\partial w}{\partial x}+v\frac{\partial w}{\partial y}+w\frac{\partial w}{\partial z}=-\frac{1}{\rho_f}\frac{\partial p}{\partial z}+\frac{\mu_f}{\rho_f}\left[\frac{\partial^2 w}{\partial x^2}+\frac{\partial^2 w}{\partial y^2}+\frac{\partial^2 w}{\partial z^2}\right] \quad (4)$$

Here, p, ρ and ν represent the pressure, density, and kinematic viscosity of the coolant, respectively. The energy equation for the fluid is expressed as follows:

$$u\frac{\partial T}{\partial x}+v\frac{\partial T}{\partial y}+w\frac{\partial T}{\partial z}=\frac{k_f}{\rho_f c_{pf}}\left[\frac{\partial^2 T}{\partial x^2}+\frac{\partial^2 T}{\partial y^2}+\frac{\partial^2 T}{\partial z^2}\right] \quad (5)$$

In this context, ρ, T, k_f and Cp denote the coolant's density, temperature, thermal conductivity, and specific heat at constant pressure, respectively.

Energy equation for the solid:

$$k_s\left[\frac{\partial^2 T}{\partial x^2}+\frac{\partial^2 T}{\partial y^2}+\frac{\partial^2 T}{\partial z^2}\right]=0 \quad (6)$$

where k_s is the thermal conductivity of the solid.

2.3. Data Analysis

The value of ΔP can be concluded as follows:

$$\Delta P = P_{in}-P_{out} \quad (7)$$

The Re is a dimensionless quantity that is defined as follows [15]:

$$Re=\frac{\rho V D_H}{\mu} \quad (8)$$

Where D_H is the hydraulic diameter of the flow channel opening and is obtained from the following equation:

$$D_H = \frac{4A}{P} \quad (9)$$

Where A is the area and P is the perimeter of the fluid inlet cross section.

This study utilizes the concept of entropy generation to evaluate heat transfer processes and flow irreversibilities across different MCHS configurations. The expressions for the total entropy generation rates are given as follows [16].

$$S_g = S_{g,\Delta p} + S_{g,\Delta T} \quad (10)$$

$$S_{g,\Delta p} = \frac{\dot{m}\Delta p}{\rho_m T_a} \quad (11)$$

$$S_{g,\Delta T} = \frac{Q_{base}\left(T_{base,avg} - T_a\right)}{T_{base,avg} T_a} \quad (12)$$

In this context, $S_{g,\Delta T}$ refers to the entropy generated due to heat transfer, while $S_{g,\Delta p}$ corresponds to the entropy produced by fluid flow. The term $\dot{m}$ denotes the mass flow rate of the fluid, and T_a is the ambient temperature, which is assumed to be equal to the inlet fluid temperature $T_{f,in}$ for this analysis.

The main purpose of the augmented entropy generation number, $N_{s,a}$ is to provide a means for comparing the irreversibility of different microchannel configurations. It is defined as follows:

$$N_{s,a} = S_g / S_{g,0} \quad (13)$$

Here, S_g denotes the entropy generation for each configuration, which is compared to that of the baseline case in the N_a formula. A value of N_a closer to zero indicates lower entropy generation and, consequently, more effective cooling performance.

3. Grid Study

Creating quality mesh has a significant impact on the results of numerical simulations. In the present study, in order to ensure the quality of the mesh, two parameters, ΔP, and average heat sink temperature, have been investigated for Case 4 at Re 600 in 4 stages. The results obtained show that the values of ΔP and heat sink temperature in the third stage (1686871 elements) have a negligible difference from the corresponding values in the fourth stage (5118750 elements). Therefore, to reduce computational costs, the third stage mesh has been selected for the investigations carried out in this study (Fig. 3).

The governing equations in the present problem have been discretized using the finite element method and COMSOL Multiphysics software. The remaining values have been considered in solving equations 10^{-5}.

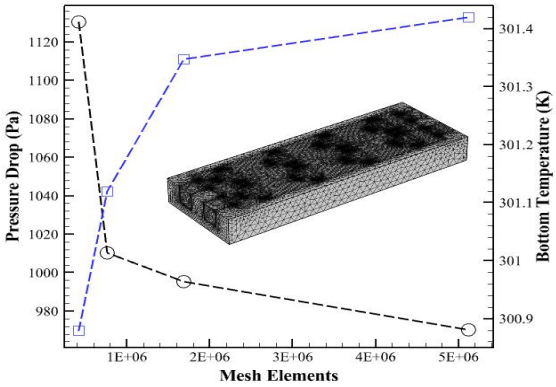

Fig. 3. Mesh information created

3.1. Validation with experimental research

To verify the results of the present work, the present numerical method has been compared with the results of Al-Hasani and Freegah [12] research. Fig. 4 clearly shows that the results obtained with the present method have a slight difference from the results of Al-Hasani and Freegah [12] work.

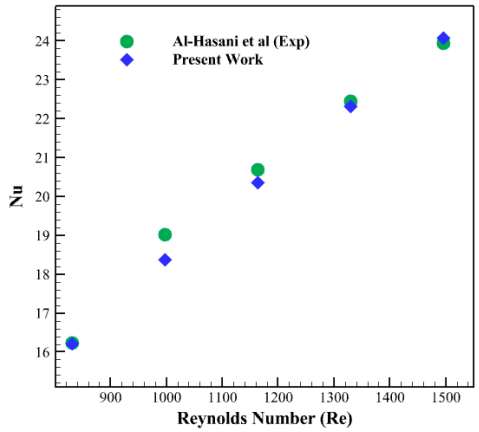

Fig. 4. Comparison of the results obtained with the numerical method compared to the work of Al-Hasani and Freegah [12].

4. Results and discussion

3.1. Impact of geometric parameters changes

The temperature distribution in the proposed cases at Re 600 is shown in Fig. 5. The comparison between the proposed cases clearly shows that adding fins with various configurations can have a significant effect on cooling and reducing the temperature of the heat sink. In the base case, due to the formation of a thermal boundary layer, little heat exchange occurs in the fluid region and most of the fluid volume with low temperature exits the heat sink and a high temperature occurs in the base case. In cases 1 to 4, by using fins in different shapes, the contact area between the solid and the fluid is increased, and more heat is transferred by the solid to the fluid. This greater heat transfer

results in better cooling and cases 1 to 4 have lower temperatures compared to the base case.

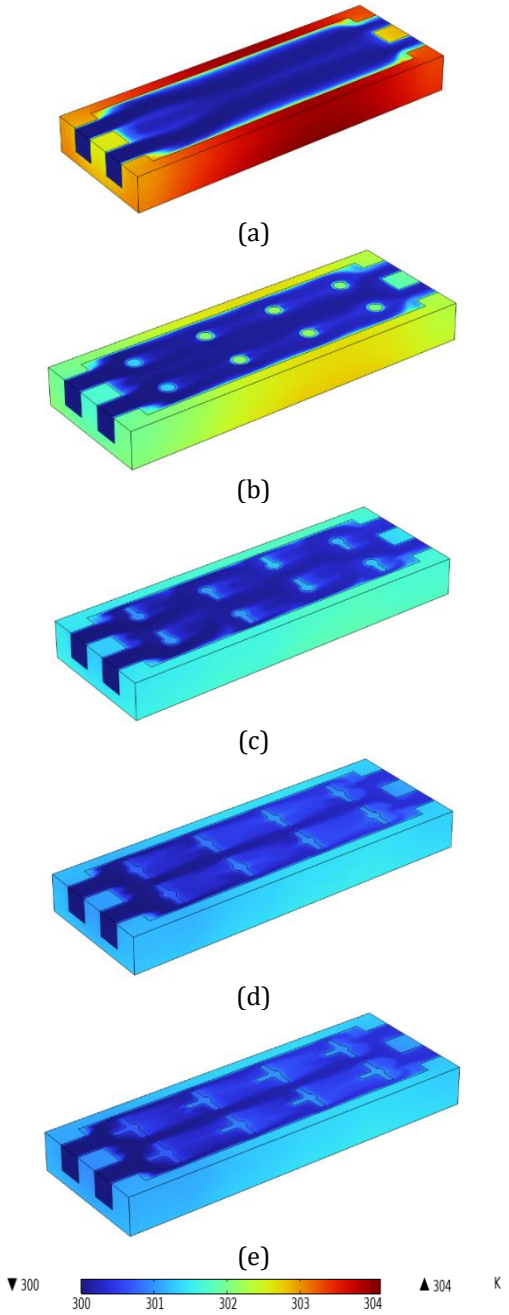

Fig. 5. Temperature distribution depicted in each case at Re = 600: (a) base case, (b) case 1, (c) case 2, (d) case 3, (e) case 4.

In this study, the changes in entropy generation (S_p) due to fluid flow have been investigated for the proposed cases in the Re range from 200 to 1000 (Fig. 6). The results show that with increasing Re, frictional forces in the fluid flow increase, and as a result, the amount of entropy production (S_p) also increases. This relationship clearly indicates the direct effect of frictional forces on entropy production in the system. In all analyses, case 3 has shown the highest S_p values among the proposed options at all Re. This finding highlights the importance of the geometry and design of case 3 in entropy generation and can be considered in optimizing similar designs.

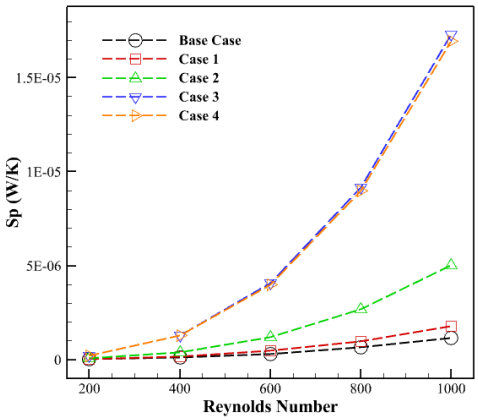

Fig. 6. Effect of geometric changes on S_p at Re = 200 to 1000.

The entropy generation changes due to heat transfer (S_t) for the proposed cases are reported in Fig. 7 from 200 to 1000. The present results show that with the increase in Re, the final result of the heat sink has decreased. In the base case on the increase in Re from 200 to 400, 600, 800, and 1000, it has decreased by 35.05%, 49.26%, 56.8% and 61.61%. In case 3, with the increase in Re from 200 to 400, 600, 800, and 1000, it has decreased by 39.17%, 53.35%, 61.09%, and 66.16%. In all Re, case 4 has the lowest compared to the rest. At Re = 200, the S_t values for Case 4 decreased by 59.86%, 41.83%, 2.45%, and 2.74% compared to the base case, Case 1, Case 2, and Case 3.

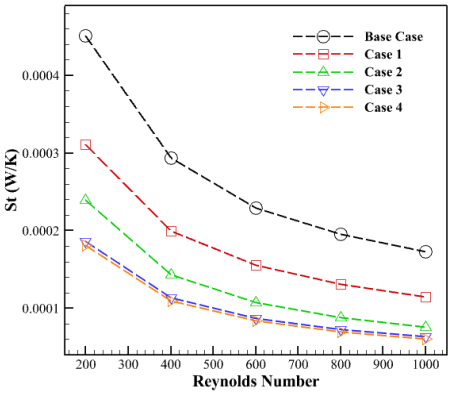

Fig. 7. Effect of geometric changes on S_t at Re = 200 to 1000.

From the perspective of the second law of thermodynamics, reducing entropy production indicates an improvement in system performance, so that the lower the amount of entropy produced, the closer that system is to the ideal state. Fig. 8 shows the entropy values produced in different cases in comparison with the base case. In this graph, the entropy values produced for the base case are considered equal

to 1 at all Reynolds numbers, and the entropy produced for all cases 1 to 4 is compared with the base case. The results show that the N_a value for cases 1 to 4 is lower than the base case, which indicates an improvement in the cooling system in cases 1 to 4. The N_a at Reynolds number 600 for case 1, case 2, case 3, and case 4 has decreased by 32.09%, 52.64%, 60.34%, and 61.86% compared to the base case. At Reynolds number 1000, the amount of N_a in Case 1, Case 2, Case 3, and Case 4 decreased by 33.36%, 53.47%, 53.97%, and 55.66%.

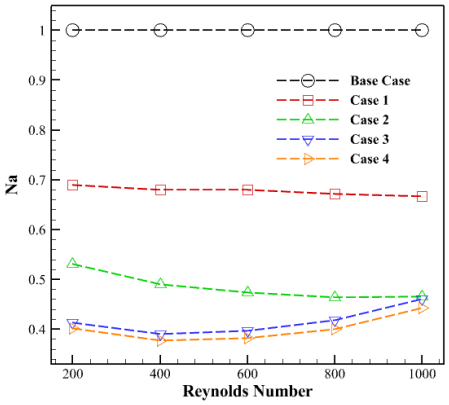

Fig. 8. Effect of geometric changes on N_a at Re of 200 to 1000

5. Conclusions

In this study, 5 different configurations for a heat sink with a constant heat flux of 20 kW/m2 are presented, and thermal and entropy analyses are performed at Re from 200 to 1000. The results show that with increasing Re, the Sp values increase and the St values decrease. Among the proposed cases, Case 4 has the lowest entropy generation in terms of the second law of thermodynamics. Some important results are given below:

- In the base case, by the increase in Re from 200 to 400, 600, 800, and 1000, S_t is decreased by 35.05%, 49.26%, 56.8%, and 61.61%.
- At Re = 200, the S_t values for Case 4 is decreased by 59.86%, 41.83%, 2.45%, and 2.74% compared to the base case, Case 1, Case 2, and Case 3, respectively.
- The N_a at Re = 600 for case 1, case 2, case 3, and case 4 is decreased by 32.09%, 52.64%, 60.34%, and 61.86%, respectively, compared to the base case.
- At Re = 1000, the amount of N_a in Case 1, Case 2, Case 3, and Case 4 decreased by 33.36%, 53.47%, 53.97%, and 55.66, respectively.

Nomenclature

Re	Reynolds Number
D_h	Hydraulic Diameter [m]
ΔP	Pressure Drop [Pa]
P	Pressure [bar]
u	Velocity in x direction [m/s]
v	Velocity in y direction [m/s]
w	Velocity in z direction [m/s]
ρ	Density [kg/m^3]
c_p	Heat Transfer Capacity [J/kg.K]
k	Thermal Conductivity [W/m.K]

References

[1] Weragoda, D.M., Tian, G., Burkitbayev, A., Lo, K.H., Zhang, T., 2023. A comprehensive review on heat pipe based battery thermal management systems. Applied thermal engineering, 224, p. 120070.

[2] Khattak, Z., Ali, H.M., 2019. Air cooled heat sink geometries subjected to forced flow: A critical review. International Journal of Heat and Mass Transfer, 130, pp. 141-161.

[3] Ghazali, M.F., Maulana, M.I., Che Sidik, N.A., Najafi, G., Mohd Rashid, M.I., Jamlos, M.F., Najafpour, A., 2024. Experimental Analysis and CFD Simulation of Photovoltaic/Thermal System with Nanofluids for Sustainable Energy Solution. Journal of Advanced Research in Numerical Heat Transfer, 24(1), pp. 1–13.

[4] Yasar, M. ., Hafsah, S., Juliaviani, N., Ghazali, M.F., Najafi , G., Rostami, M.H., Najafpour, A., 2024. CFD Simulation of Solar Dish Concentrator with Different Cavity Receivers. Journal of Advanced Research in Numerical Heat Transfer, 25(1), pp. 1–12.

[5] Maulana, M.I., Ghazali, M.F., Abdullah , A., Che Sidik, N.A., Najafi, G., Najafpour, A., 2024. Optimizing Solar Dish Concentrator Efficiency with Nanofluids and Diverse Cavity Design. Journal of Advanced Research in Numerical Heat Transfer, 25(1), pp. 87–99.

[6] Luo, J., Zou, D., Wang, Y., Wang, S., Huang, L. (2022). Battery thermal management systems (BTMs) based on phase change material (PCM): A comprehensive review. *Chemical Engineering Journal*, *430*, 132741.

[7] Gao, Y., Wang, C., Wu, D., Dai, Z., Chen, B., Zhang, X., 2022. A numerical evaluation of

the bifacial concentrated PV-STEG system cooled by mini-channel heat sink. Renewable Energy, 192, pp. 716-730.

[8] Deng, Z., Zhang, S., Ma, K., Jia, C., Sun, Y., Chen, X., Li, T., 2023. Numerical and experimental study on cooling high power chips of data centers using double-side cooling module based on mini-channel heat sink. Applied Thermal Engineering, 227, p. 120282.

[9] Gunnasegaran, P., Mohammed, H.A., Shuaib, N. H., Saidur, R., 2010. The effect of geometrical parameters on heat transfer characteristics of microchannels heat sink with different shapes. International communications in heat and mass transfer, 37(8), pp. 1078-1086.

[10] Najafpour, A., Hosseinzadeh, K., Kermani, J. R., Ranjbar, A.A., Ganji, D.D., 2024. Numerical study on the impact of geometrical parameters and employing ternary hybrid nanofluid on the hydrothermal performance of mini-channel heat sink. Journal of Molecular Liquids, 393, p. 123616.

[11] Ghadhban, F.N., Jaffal, H.M., 2023. Numerical investigation on heat transfer and fluid flow in a multi-minichannel heat sink: Effect of channel configurations. Results in Engineering, 17, p. 100839.

[12] Al-Hasani, H.M., Freegah, B., 2022. Influence of secondary flow angle and pin fin on hydro-thermal evaluation of double outlet serpentine mini-channel heat sink. Results in Engineering, 16, p. 100670.

[13] Najafpour, A., Montazer, E., Hosseinzadeh, K., Ranjbar, A.A., Ganji, D.D., Kanesan, J., 2024. Computational study on the impact of geometric parameters on the overall efficiency of multi-branch channel heat sink in the solar collector. International Communications in Heat and Mass Transfer, 158, p. 107884.

[14] Najafpour, A., Rostami, M.H., 2025. Numerical analysis of thermal and hydrothermal characteristics of a heat sink with various fin configurations and ternary nanofluid composition. Case Studies in Thermal Engineering, 68, p. 105928.

[15] Najafpour, A., Hosseinzadeh, K., Akbari, S., Mahboobtosi, M., Ranjbar, A.A., Ganji, D.D. (2023). Numerical study of mixing performance in T-junction passive micromixer with twisted design. Chemical Engineering and Processing-Process Intensification, 194, p. 109567.

[16] Feng, Z., Luo, X., Guo, F., Li, H., Zhang, J., 2017. Numerical investigation on laminar flow and heat transfer in rectangular microchannel heat sink with wire coil inserts. Applied Thermal Engineering, 116, p. 597-609.